Supplementary Information

In vivo detection of Staphylococcus aureus endocarditis by targeting pathogen-specific prothrombin activation

Peter Panizzi[1,2,3], PhD; Matthias Nahrendorf[1,3], MD, PhD; Jose-Luiz Figueiredo[1], MD; Jennifer Panizzi[4], PhD; Brett Marinelli[1], Yoshi Iwamoto[1], Edmund Keliher[1], PhD; Ashoka A. Maddur[6], PhD; Peter Waterman[1]; Heather K. Kroh[6], PhD; Florian Leuschner MD; Elena Aikawa[1], MD, PhD; Filip K. Swirski[1], PhD; Mikael J. Pittet[1], PhD; Tilman M. Hackeng[5], PhD; Pablo Fuentes-Prior[7], PhD; Olaf Schneewind[8], MD PhD; Paul E. Bock[6], PhD; and Ralph Weissleder[1,9], MD, PhD

[1]Center for Systems Biology, Massachusetts General Hospital and Harvard Medical School, Simches Research Building, 185 Cambridge St., Boston, MA 02114, USA; [2]Department of Pharmacal Sciences, Harrison School of Pharmacy, Auburn University, Auburn, AL 36849 USA; [4]Nephrology Division, Massachusetts General Hospital, Charlestown, MA, 02129 USA; [5]Department of Biochemistry, Cardiovascular Research Institute Maastricht, University Maastricht, Universiteitssingel 50, 6229 ER Maastricht, The Netherlands; [6]Department of Pathology, Vanderbilt University School of Medicine, Nashville, TN, 37232 USA; [7]Institut de Recerca, Hospital de la Santa Creu i Sant Pau, Sant Antoni Maria Claret 167, 08025 Barcelona, Spain; [8]Department of Microbiology, The University of Chicago, Chicago, IL 60637 USA; [9]Department of Systems Biology, Harvard Medical School, Boston, MA 02115, USA

Corresponding author: Matthias Nahrendorf and Ralph Weissleder
mnahrendorf@mgh.harvard.edu
rweissleder@mgh.harvard.edu

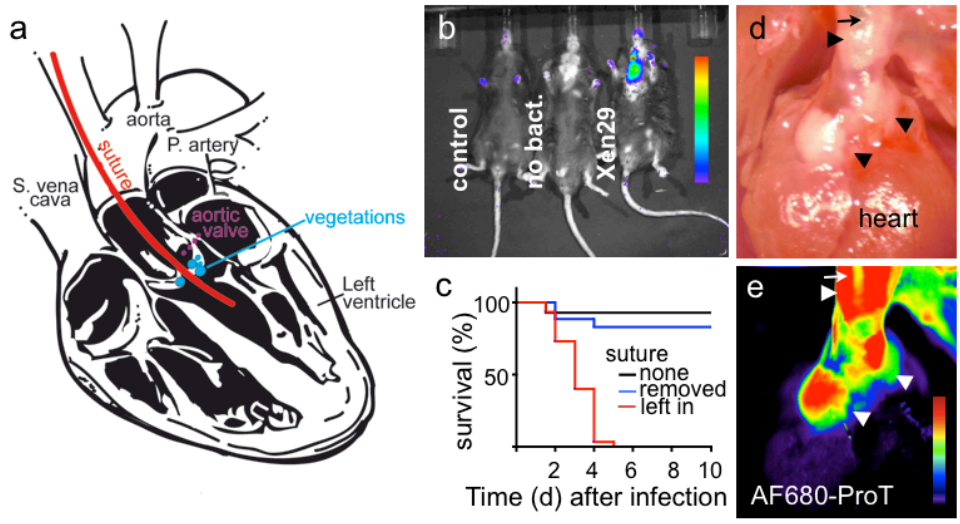

Supplementary Figure 1. Mouse model of staphylococcal endocarditis. (**a**) Diagram demonstrating placement of the suture material (*red*) through the aortic valve. (**b**) Bioluminescence imaging of naive mice (*left*), mice with the suture inserted (*middle*), and mice with the suture inserted and after intravenous injection of *S. aureus* Xen29 (*right*). (**c**) Kaplan-Meier curves comparing the mortality associated with the absence (*black*) or presence of the suture material, and the survival rate when the suture is left in place (*red*) or when immediately removed after placement (*blue*). Here, all cohorts were injected with *S. aureus* Xen29. (**d**) Representative *in situ* image of vegetations formed in the aorta (marked by arrow heads) near the aortic root. The suture is marked by the arrow. (**e**) Fluorescence image of the same mouse visualizes AF680-ProT localization in vegetations.

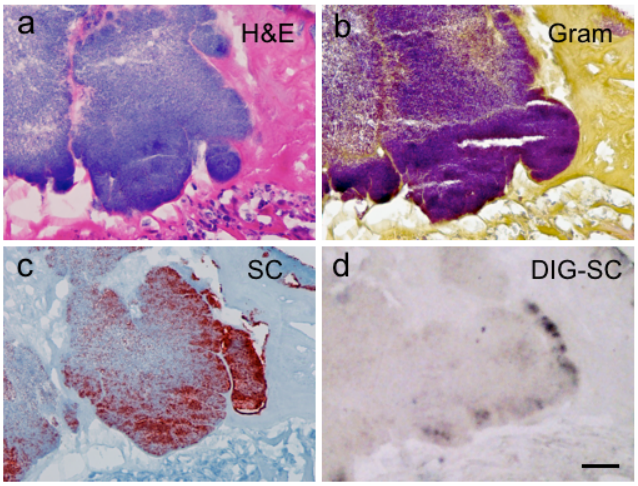

Supplementary Figure 2. Staphylocoagulase localization at the host-pathogen interface. Adjacent sections are shown for H&E (**a**), Gram (**b**), and SC immunohistochemistry staining (**c**), as well as *in situ* hybridization against digoxigenin-SC RNA (DIG-SC) (**d**). Distance bar equals 50 μm.

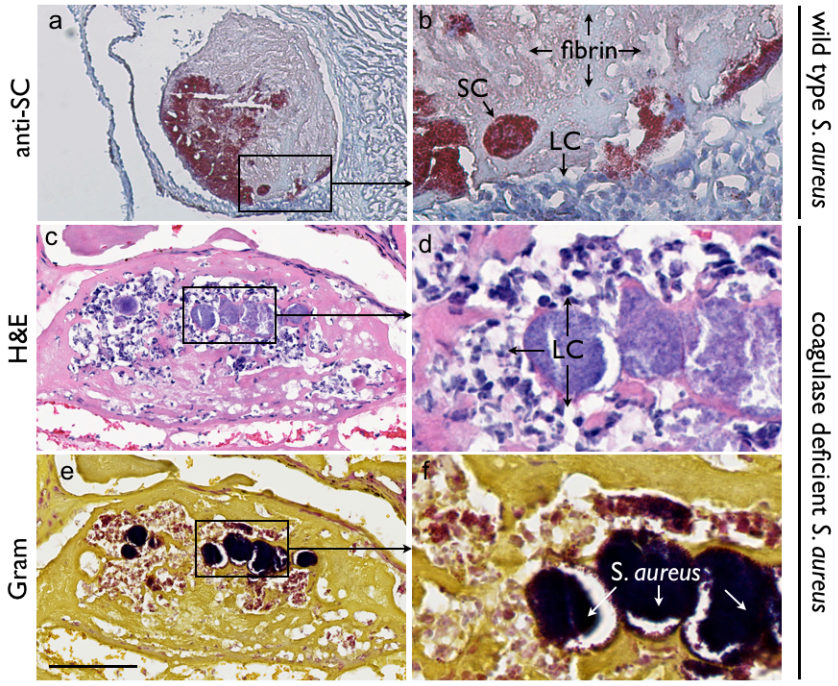

Supplementary Figure 3. Infiltration of endocarditis vegetations by leukocytes in mice injected with *S. aureus* deficient in coagulase activity. (**a,b**) In a younger wild type vegetation, that only occupies a single aortic valve leaflet, SC is located thoughout the entire vegetation. (**c-f**) Histology in mice infected with coagulase deficient *S. aureus.* H&E (**c, d**) and Gram staining (**e, f**) indicate the absence of a fibrin barrier. Instead, leukocytes (LC) are present inside the vegetation, which is not typical for coagulase-producing *S. aureus* strains (compare to panels a, b and to Figure 1a-d). The bar represents 100 µm.

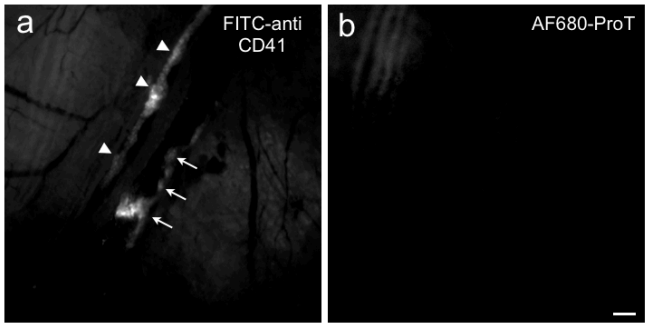

Supplementary Figure 4. AF680-ProT does not bind to femoral artery thrombosis. To test for specificity, we injected AF680-ProT into mice with thrombosis but without bacteremia. (**a**) Fluorescence image of a FITC-labeled antibody against CD41 after injury of the femoral vessels with ferric chloride. The location of the thrombus was confirmed by injection of this fluorescently labeled antibody that binds to activated platelets. Fluorescent clots were detected in both, the femoral artery (arrow heads) as well as in the femoral vein (arrows). (**b**) Fluorescence image obtained in the near infrared indicated the lack of AF680-ProT accumulation in the thrombus. Experiment was done in duplicates, distance bar represents 1 mm.

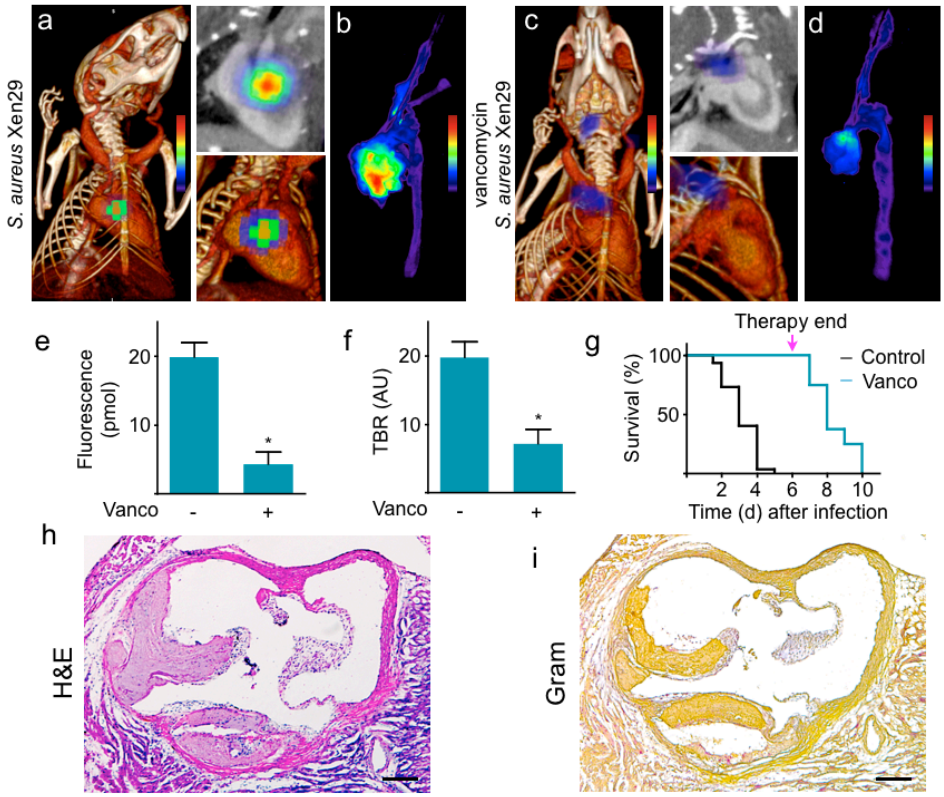

Supplementary Figure 5. AF680-ProT monitors therapeutic efficacy of vancomycin in *S. aureus* endocarditis. Representative FMT-CT images (**a**) and *ex vivo* FRI images of dissected aortas (**b**) are shown for a mouse injected with AF680-ProT and *S. aureus* Xen8.1, and for similar mice treated daily with vancomycin (**c,d**). Total fluorescence concentration of AF680-ProT obtained by in vivo FMT-CT (**e**) and target-to-background ratio (TBR) of ex vivo FRI (**f**) for respective groups are shown. (**g**) Survival curves for mice with endocarditis, with and without daily vancomycin treatment. Treatment was terminated on day 6 causing reemergence of the infection. n=8-10 per group, *p<0.01. (**h**) H&E and (**i**) Gram stain of an aortic valve with endocarditis vegetations, after 6 days of treatment with vancomycin. The images indicate that the treatment eliminated bacteria in vegetations. Bar equals 100 μm.

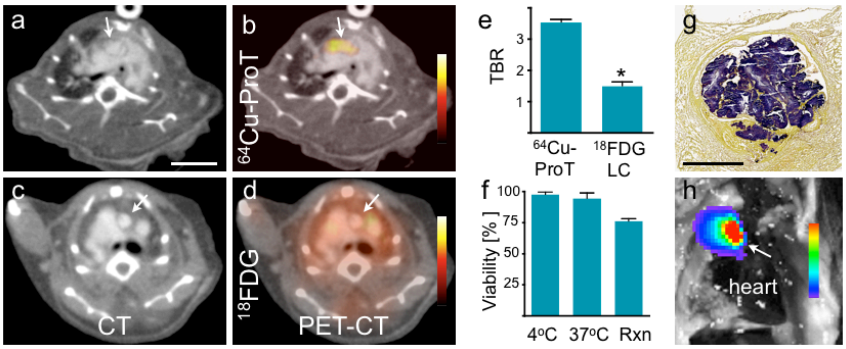

Supplementary Figure 6. Comparison of ^{64}Cu-ProT and ^{18}FDG-labeled leukocyte PET-CT (^{18}FDG LC) for detection of *S. aureus* endocarditis. Representative axial views are shown for mice with endocarditis imaged by PET-CT (**a-d**). Arrows denote the aortic valve and fused PET signal is shown for ^{64}Cu-ProT (**b**) or ^{18}FDG-labeled leukocytes (**d**). (**e**) Target to background ratio (vegetation / blood TBR, n=5, *p<0.05). (**f**) Viability of leukocytes labeled with ^{18}FDG (Rxn) is shown alongside leukocytes maintained on ice (4ºC) and those that were incubated at 37ºC. Endocarditis was confirmed by Gram staining of the aortic valve (**g**) and *in situ* bioluminescence (**h**, arrow). Bar indicates 0.5 mm.

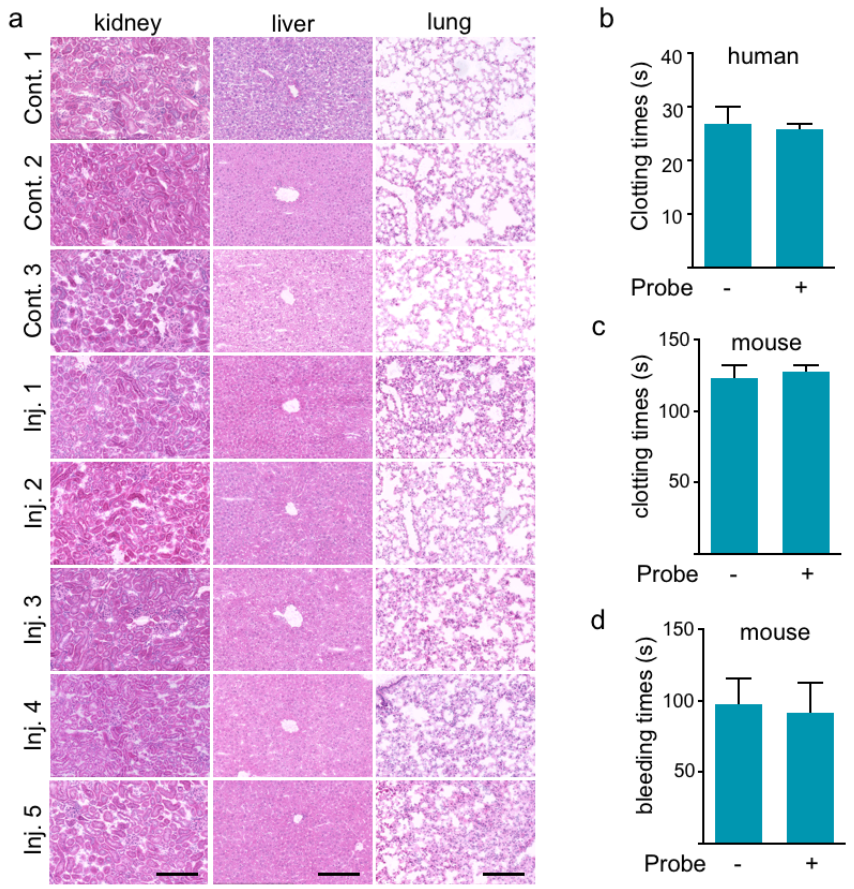

Supplementary Figure 7. Prothrombin analog toxicity study. (**a**) H&E staining of tissue sections from mice that were injected with prothrombin analog (Inj. 1-5) after three doses (250µg, corresponding to 10X imaging dose) over a week, and uninjected control mice (Cont. 1-3). No abnormalities such as inflammatory foci, necrosis, clots or bleeding were observed. Bar represents 200 µm. (**b-d**) Prothrombin analog clotting studies. Prothrombin times are shown for either human (**b**) or mouse (**c**) plasma incubated with 250µg prothrombin analog at 37°C. A tail tip bleeding assay (**d**) compared control mice to those injected with 10 times the imaging dose of prothrombin analog. The data (n=5 per group) showed no significant differences in clotting parameters after injection of the probe.

Enzyme	k_{cat} (s^{-1})	K_m (μM)	k_{cat}/K_m ($\mu M^{-1}s^{-1}X10^{-3}$)	K_i (μM)
human thrombin[1]	77 ± 1	2.5 ± 0.2	31000	11.5 ± 0.2
SC•human prothrombin[1]	72.2 ± 0.1	1.2 ± 0.1	58000	6.2 ± 0.1
mouse thrombin	26 ± 1	1.46 ± 0.3	18000	7.5 ± 1.1
SC•mouse prothrombin	26 ± 1	14.2 ± 0.1	1800	163 ± 80
bovine thrombin[2]	94 ± 2	3 ± 1	35000	32 ± 2
SC•bovine prothrombin[2]	1.4 ± 0.1	140 ± 50	10	

Supplementary Table 1. Species-specificity of SC-(1-325) binding to prothrombin. Michaelis-Menten kinetic parameters determined for hydrolysis of H-*D*-Phe-Pip-Arg-*p*NA by the indicated enzyme species are listed. Parameters were obtained by nonlinear least-squares fitting of the integrated equation to progress curves for mouse prothrombin in the presence of saturating concentrations of SC-(1-325) and mouse thrombin alone. Kinetic parameters previously determined in respective references are listed for comparison.

Supplementary Methods

Bacterial strains. *Staphylococcus aureus (S. aureus)* strains Newman D2 Tager 104, Xen29 and Xen8.1 are vancomycin-susceptible strains. Bioluminescent *S. aureus* Xen29 and Xen8.1 were purchased from Caliper Inc. *S. aureus* strain Newman D2 Tager 104 was obtained from Stago Inc., and *S. epidermidis* FDA strain PCI 1200 was obtained from ATCC. Newman SC and VWbp double knockout *S. aureus* strain were prepared by allelic replacement in *Staphylococcus aureus* with temperature dependent shift using a modified pKOR1 shuttle plasmid[3]. Bacterial strains were grown to log phase overnight in heart-brain infusion media (Sigma-Aldrich). The bacteria were centrifuged to remove media, washed twice with PBS, and diluted (immediately prior to injection) to a concentration of 1 x 10^7 colony forming units (CFUs) / ml. To standardize the number of bacteria injected, all strains were supplemented with 10% glycerol and stored at -80º C in single-use aliquots. To verify the number of bacteria injected, a portion of the inoculums was plated onto heart-brain infusion agar, from which CFUs were determined.

Native Gel Band Shift Experiments. Purified proteins or mixtures as indicated in Figure 2 were incubated at room temperature for 20 min in the presence of 100 μM D-Phe-Pro-Arg-CH_2Cl before addition of gel treatment buffer. Non-denaturing or native gel electrophoresis was performed with 10% polyacrylamide gels (Bio-Rad) using running buffer excluding both sodium dodecyl sulfate and 2-mercaptoethanol.

Activation of mouse prothrombin by staphylocoagulase (SC). Owing to the species-specific nature of ProT activation by different SC strains[2], it was necessary to initially determine whether mouse prothrombin was activated by SC expressed by the *S. aureus* strains used to develop *S. aureus* endocarditis. An active fragment of staphylocoagulase (SC(1-325)) from *S. aureus* Newman D2 Tager 104 (NCBI accession number AAO65980) had been previously cloned and over-expressed in *E. coli* [1,4]. Mouse ProT activation by SC(1-325) was determined in kinetic studies using a chromogenic tripeptide thrombin substrate. SC-prothrombin activity titrations were measured from progress curves of 100 μM H-*D*-Phe-Pip-Arg-*p*-nitroanilide hydrolysis at

405 nm in 50 mM HEPES (4-(2-hydroxyethyl)-1-piperazineethanesulfonic acid), 110 mM NaCl, 5 mM $CaCl_2$, 0.1 mg ml^{-1} soybean trypsin inhibitor, 1 mg ml^{-1} bovine serum albumin (BSA), pH 7.4 at 25 °C. Michaelis–Menten kinetic parameters were determined by simultaneous fits of these substrate-depletion progress curves.

Preparation of SC PR-R1[5F]. The pseudorepeat–repeat 1 (PR-R1) construct was amplified by PCR using an existing SC(1-660) construct (Tiger strain 104) and ligated into a modified pET30b(+) (Novagen) expression vector[1]. Forward and reverse primers were: 5'-GCGAGACCTCAATTTAACAAAACACCT-3' and 5'-CCCATATGATACTTGGCCGTTTGCATG-3', respectively. A COOH-terminal Cys residue was introduced by QuikChange site-directed mutagenesis and confirmed by DNA sequencing. PR-R1-Cys expression was induced by lactose in Rosetta 2 (DE3) pLysS *E. coli* in the presence of 0.1 mg/ml of kanamycin. The cells were lysed by three freeze-thaw cycles, and the protein present in the inclusion bodies was resolubilized in buffer containing 3 M NaSCN. The solution was dialyzed against 50 mM HEPES, 325 mM NaCl, 50 mM imidazole, pH 7.4 before chromatography on Ni^{2+}-iminodiacetic acid-Sepharose and elution with a gradient of 0–500 mM imidazole. The NH_2-terminal His_6-tag was removed by incubation with tobacco etch virus proteinase at a 1:10 molar ratio for 12-14 h and subsequent Ni^{2+}-iminodiacetic acid-Sepharose chromatography[1]. Purified PR-R1-Cys was reduced with 1 mM dithiothreitol (DTT) and dialyzed extensively against 5 mM MES, 150 mM NaCl, pH 6.0. PR-R1-Cys concentration was determined from the absorbance at 280 nm, with an absorption extinction coefficient of 1.17 ($(mg/ml)^{-1}$ cm^{-1}) and a molecular mass (Da) of 8483. Thiol incorporation measured with 5,5'-dithiobis-(2-nitrobenzoic acid) was 0.97 mol Cys / mol PR-R1-Cys. For labeling, the pH of 25 μM PR-R1-Cys was raised to ~7 by addition of 0.1 volume 1 M Hepes, pH 7.0 and incubated with 5-fold molar excess of 5-(iodoacetamido)fluorescein for 12 -14 h at 4 °C. The reaction was quenched with 1 mM DTT and centrifuged for 15 min at 10,600 x g, then excess probe was removed by extensive dialysis against 50 mM HEPES, 125 mM NaCl, pH 7.4. Incorporation of label was determined by measurements of absorbance at 280 nm and 498 nm, with an absorption coefficient of 84,000 M^{-1} cm^{-1} for fluorescein at 498 nm and an $A_{280\ nm}/A_{498\ nm}$ ratio of 0.19 in 6 M

guanidine, 100 mM Tris-Cl, 1 mM EDTA, pH 8.5[5]. The final labeling ratio was 1.1 mol fluorescein/mol PR-R1[5F].

Equilibrium Binding of PR-R1[5F] to FragD. Fluorescence titrations were performed with excitation at 490 nm (2-4 nm band pass), emission at 517 nm (4-8 nm band pass), in 50 mM HEPES, 110 mM NaCl, 5 mM $CaCl_2$, 1 mg/ml polyethylene glycol 8000, pH 7.4 at 25 °C.

Molecular modeling of DTPA-ProT-SC complex. To assess the potential accessibility of the chelator, a three-dimensional molecular model was developed using SC(1-325)•prethrombin 2 as a template (Protein Data Bank accession code 1NU9; [1]). For generating the active site-bound chelator, we used structures of (a) the TLR2 and TLR6 ectodomain heterodimers bound to 1,2-dimyristoyl-*sn*-glycero-3-phosphoethanolamine (PE)-DTPA (PDB 3A7C)[6], and (b) a variant of the neutrophil gelatinase-associated lipocalin complexed with [(*R*)-2-amino-3-(4-aminophenyl)propyl]-*trans*-(*S*,*S*)-cyclohexane-DTPA (PDB 3DSZ)[7]. The bound lutetium(III) / ytterbium(III) ions were replaced with a Cu^{2+} ion, according to distances with coordinating atoms for Cu(II)-DTPA monohydrate[8]. Because the protected thiol on the N^{α}-[(acetylthio)acetyl]-D-Phe-Pro-Arg-CH_2Cl linker was the same for both labeling strategies, the two alternative positions observed for the Hg atom in 1NU9 could be used as reference to orient the DTPA chelator. Orientation following the secondary Hg position located the chelator closer to the active site cleft, roughly at the same distance to the 60- and 149-loops (Figs. 5a & 5b). The DTPA moiety would most likely be free to oscillate with minimal steric hindrance.

Synthesis of AF680-ProT and ^{64}Cu-DTPA-ProT. Active-site inactivated human prothrombin derivatives were generated through the use of the thioester peptide chloromethyl ketone, N^{α}-[(acetylthio)acetyl]-D-Phe-Pro-Arg-CH_2Cl. The activator-zymogen complex was formed, generating an active site that was inactivated by the addition of N^{α}-[(acetylthio)acetyl]-D-Phe-Pro-Arg-CH_2Cl. The protected thiol was then liberated by addition of 1 M hydroxlyamine (0.1/1 vol/vol) in the presence of the thiol-

reactive labeling reagent, Alexa Fluor 680 C_2 maleimide (Invitrogen) or maleimide-functionalized diethylenetriaminepentaacetic acid (DTPA-maleimide). The activator was removed by nickel affinity chromatography by elution of either AF680-ProT or DTPA-ProT with 3 M sodium thiocyanate. 2-{{bis-{2-[bis-(carboxymethyl)amino]-ethyl}-amino}}-6-(1-maleimido-3-carbonyl-aminophenyl) hexanoic acid (DTPA-maleimide) was prepared as described previously[9]. Because the residual active prothrombin in the final product could trigger downstream activation of the clotting cascade, we determined its concentration in each batch of labeled prothrombin analogs used. AF680-ProT or ^{64}Cu-DTPA-ProT had residual activities of 0.3 and 0.2%, respectively.

^{64}Cu-DTPA-ProT was prepared by incubation of 225 µg in 84 µL of PBS with 15.48 mCi of $^{64}CuCl_2$ in 30 µL ammonium acetate buffer (0.4 M, pH 6.5) at 40 ^{o}C for 1 hour. After cooling to room temperature, the reaction mixture was transferred to a centrifuge filter (50 kDa, Millipore), diluted with 100 µL PBS and centrifuged to remove unbound ^{64}Cu. This dilution and concentration step was repeated 4 times until no activity was measured in the filtrate. ^{64}Cu-DTPA-ProT (8.87 mCi) collected on the filter was diluted in 200 µL PBS and transferred to a vial to prepare syringes for tail vein injection into mice.

Fluorescence reflectance imaging and histology. Following infection with *S. aureus* and FMT-CT imaging, the aortas were excised. The samples were imaged side-by-side with controls with an epifluorescence microscope (OV-110, Olympus). The tissue was then fixed in 4% paraformaldehyde (PFA) for at least 12 hours, embedded in OCT, and flash-frozen in an isopentane/dry ice bath. H&E and Gram staining (Sigma-Aldrich) were performed to verify the presence of *S. aureus* bacteria on the aortic valve. Fluorescence microscopy (Eclipse 80i, Nikon) was performed to investigate microscopic AF680-ProT localization in the vegetation. Immunohistochemistry for SC and VWbp was performed using polyclonal antibodies generated against SC(13-325) and VWbp (2-474) (OpenBiosystems, Inc.). The recombinant proteins used to generate the polyclonal antibodies for either the SC or VWbp fragments lacked NH_2-terminal residues. This minimized any toxicity resulting from systemic prothrombin activation. A

biotinylated secondary antibody, ABC kit (Vector Laboratories, Inc.), and AEC substrate (DakoCytomation) were used for the color development and all the sections were counterstained with Harris hematoxylin.

***In situ* hybridization for SC.** SC(1-660) (NCBI accession number AAO65980) was subcloned into pCRII-TOPO (Invitrogen; a dual promoter vector that contains both SP6 and T7 promoters) following digestion of the original clone with NcoI and XhoI in the pET30b(+) vector, and after brief incubation with dATP and Taq polymerase. Directionality of the gene was confirmed by DNA sequencing (MGH DNA sequencing core). The antisense probe was synthesized using T7 polymerase and digoxigenin-labeled-UTP (Roche) following digestion of the template with BamHI. The sense probe was synthesized using SP6 polymerase and DIG-labeled-UTP. OCT-embedded 6-8 micron PFA-fixed cryosections were washed in PBS, before lysostaphin (0.1 µg/ml) and lysozyme (2 mg/ml) were added for 30 minutes at 25 °C. This was followed by a 10 minute fixation in 4% PFA. Sections were washed in PBS before addition of hybridization buffer (50% formamide, 5x saline-sodium citrate (SSC; 75 mM sodium citrate, 750 mM NaCl, pH 7.0), 50 µg/ml heparin, 500 µg/ml tRNA, pH 6.0 (adjusted with citric acid) and incubation at 65 °C for 30 min. Fresh hybridization buffer with 150 ng of probe was added to each section and incubated overnight at 65 °C. After probe removal, sections were washed for 10 minutes in 5xSSC at 65 °C followed by 3 times for 30 min in 0.2xSSC (3 mM sodium citrate, 30 mM NaCl, pH 7.0) at 65 °C. Sections were subsequently washed at room temperature in 0.2xSSC for 5 min, then in PBS for 5 min, followed by antibody blocking buffer (PBS, 2% goat serum, 2 mg/ml BSA) for 1 h. Anti-digoxigenin-AP-Fab fragments (Roche) were added at 1:3000 dilution in blocking buffer, and incubated on sections at 4 °C overnight. Following 4-10 min washes in PBS, sections were incubated briefly in staining buffer (100 mM Tris-Cl, pH 9.5, 50 mM $MgCl_2$, 100 mM NaCl), then with staining buffer plus nitroblue tetrazolium (225 µg/ml) and 5-bromo-4-chloro-3-indolyl phosphate (175 µg/ml), until color developed. Reactions were stopped by addition of PBS, pH 5.5, 1 mM ethylenediaminetetraacetic acid solution. Slides were then briefly drained and stored at 4 °C following the addition of Permount and coverslips.

Monitoring of antibiotic therapy. To image the efficacy of AF680-ProT for monitoring vancomycin therapy, endocarditis was induced in 4 cohorts (n = 8-10 mice per group). Mice received daily intraperitoneal injections of 10 µg vancomycin (RPI) or PBS (Lonzo) for 6 days. For imaging, 2 groups were imaged at 48 hours post infection by FMT-CT and subsequently sacrificed for *ex vivo* fluorescence imaging of excised aortas. FRI was performed on an OV-110 epifluorescence microscope (Olympus) on all groups simultaneously to allow for side-by-side comparison of signal intensity of treated *versus* non-treated samples. Survival was then assessed in 2 additional cohorts.

PET-CT imaging of ^{18}F-FDG labeled leukocytes in *S. aureus* endocarditis. Mouse leukocytes were labeled with ^{18}F-FDG (PETNET) by incubation at 37 °C for 30 min.[10] [^{18}F]-2-Deoxy-2-fluoro-D-glucose (^{18}F-FDG) (16.7 mCi, 618 MBq, PETNET) was added to isolated leukocytes (20 million) in phosphate buffered saline supplemented with 0.5% BSA, 1% fetal calf-serum in a total volume of 1.25 ml. The reaction was incubated at 37 °C for 40 min with gentle mixing of the tube every 5 min. The reaction was stopped by washing 3 times the afore mentioned buffer with cells separated by centrifugation (300 x g for 8 min). The cells were pelleted, resuspended, and counted by hemocytometer and prepared for injection in a final volume of 300 µL cell suspension containing 1726 µCi ^{18}F-FDG in 15-17 million cells. Labeled cells were then injected into infected mice and imaged 1 h thereafter by PET-CT (n=6).

Femoral artery thrombosis imaging. Thrombosis imaging experiments[11] were done to investigate the specificity of AF680-ProT for endocarditic vegetations that contain SC. In mice injected with FITC-labeled CD41 (a maker for platelet activation), $FeCl_3$ soaked filter paper slices (500mM $FeCl_3$ solution) were placed onto isolated femoral arteries for 5 minutes. One hour later, mice were injected with AF680-ProT (25 µg). The induced clots were imaged with an intravital microscope (OV110 system, Olympus) for presence of activated platelets in the GFP channel and unspecific binding of AF680-ProT in the near infrared.

Toxicity. We performed screening studies on 5 mice injected intravenously with a dose that represents 10 times the amount of AF680-ProT used for the imaging study to determine whether there are signs of toxicity. This 10-fold dose (250 μg) was injected 3 times over a week. Tissue from liver, kidney, and lung was harvested and processed for histology. H&E staining was compared to tissue of control mice that did not receive the agent. We specifically screened for focal inflammation, liver necrosis, and thrombotic events.

Clotting studies. To address a potential concern that the inactive prothrombin (represented by the probe) may interfere with the normal activation of fibrinogen, we performed several clotting assays. Probe (30 μg) was added to 2 ml of either mouse or human plasma (Innovative Research) and prothrombin times were determined by using a BBL fibrosystem fibrometer. Clotting was initiated by the addition of thromboplastin C. In vivo clotting assays, including tail tip bleeding time, were performed in 5 C57BL/6 mice injected with AF680-ProT at 10 times the imaging dose 3 times over a week.

References for Supplementary Information

1. Panizzi, P.*, et al.* Novel fluorescent prothrombin analogs as probes of staphylocoagulase-prothrombin interactions. *J. Biol. Chem.* 281, 1169-1178 (2006).
2. Friedrich, R.*, et al.* Structural basis for reduced staphylocoagulase-mediated bovine prothrombin activation. *J. Biol. Chem.* 281, 1188-1195 (2006).
3. Cheng A.G., *et al.* Contribution of Coagulases towards *Staphylococcus aureus* Disease and Protective Immunity. *PLoS Pathog.* 6(8), (2010).
4. Friedrich, R.*, et al.* Staphylocoagulase is a prototype for the mechanism of cofactor-induced zymogen activation. *Nature* 425, 535-539 (2003).
5. Bock, P. Active-site-selective labeling of blood coagulation proteinases with fluorescence probes by the use of thioester peptide chloromethyl ketones. I. Specificity of thrombin labeling. *J. Biol. Chem.* 267, 14963-14973 (1992).
6. Kang, J.Y.*, et al.* Recognition of lipopeptide patterns by Toll-like receptor 2-Toll-like receptor 6 heterodimer. *Immunity* 31, 873-884 (2009).
7. Kim, H.J., Eichinger, A. & Skerra, A. High-affinity recognition of lanthanide(III) chelate complexes by a reprogrammed human lipocalin 2. *J. Am. Chem. Soc.* 131, 3565-3576 (2009).

8. Fomenko, V.V., Polynova, T.N., Porai-Koshits, M.A., Varlamova, G.L. & Pechurova, N.I. Crystal structure of copper (II) diethylenetriaminepentaacetate monohydrate. *J. Struct. Chem.* 14, 529 (1973).
9. Dirksen, A., Meijer, E.W., Adriaens, W. & Hackeng, T.M. Strategy for the synthesis of multivalent peptide-based nonsymmetric dendrimers by native chemical ligation. *Chem. Commun. (Cambridge, England)*, 1667-1669 (2006).
10. Dumarey, N.*, et al.* Imaging infection with 18F-FDG-labeled leukocyte PET/CT: initial experience in 21 patients. *J. Nucl. Med.* 47, 625-632 (2006).
11. Berny M.A., *et al*. Spatial distribution of factor Xa, thrombin, and fibrin(ogen) on thrombi at venous shear. *PLoS One*. 5, e10415 (2010).